IM-19: a new flexible microporous gallium based-MOF framework with pressure- and temperature-dependent openings†

Gérald Chaplais,*[a] Angélique Simon-Masseron,[a] Florence Porcher,*[bc] Claude Lecomte,[c] Delphine Bazer-Bachi,[d] Nicolas Bats[d] and Joël Patarin[a]

Received 11th December 2008, Accepted 1st April 2009
First published as an Advance Article on the web 24th April 2009
DOI: 10.1039/b822163d

Five metal–organic frameworks (MOFs) based on the same three-dimensional gallium terephthalate network (IM-19) are described, and an incommensurate structure (for the as-synthesized form) as well as two remarkable guest-free polymorphs (open and closed) are highlighted.

Within the last fifteen years, the development of a new class of organic–inorganic hybrid compounds, the coordination polymers, also called metal–organic frameworks (MOFs), has widely increased. Such solids are synthesized from metal and organic sources, usually at low temperature, and give rise to one-dimensional, two-dimensional or three-dimensional structures where the inorganic sub-network is made up of clusters, chains, layers or even three-dimensional networks. The tremendous interest in this family of solids can be related to the potential porous nature of these materials (for some MOFs, the reported values for the Langmuir surface area are higher than 3500 $m^2\ g^{-1}$ such as MOF-5,[1,2] IRMOF-20,[2,3] MOF-177,[2,4–6] MIL-101[7–11] and PCN-6[12]). Their porous characteristic make MOFs good candidates for host–guest chemistry, such as in gas and liquid adsorption, separation, storage, catalysis or as nanoreactors.[13] Surprisingly, relatively few gallium-based phosphonates,[14–23] or even rarer, carboxyphosphonates[24] and carboxylates[25–27] have been reported even though this metal is known to be incorporated in a large variety of structures in zeolites and related materials.[28,29] Compared to zeolites and related materials, the structural flexibility constitutes one of the specific properties of MOFs. Férey and co-workers have prepared a series of MOFs named MIL-53(Al, Cr)[30–32] and MIL-47(V)[33] illustrating this "breathing" behavior and have been classified as type V flexible coordination polymers by Kitagawa and Uemura.[34]

Herein, gallium-based components of this family (IM-19 hybrids) are described. The structural flexibility of the Ga(OH)(BDC) framework (BDC: terephthalate group) towards the nature of guest species (guest molecules: H_2BDC, DMF, H_2O with H_2BDC = $HO_2C–C_6H_4–CO_2H$ or terephthalic acid) will be discussed. We also present two different guest-free forms (open or closed) which are temperature- and pressure-dependent. One of these hybrids (MOF with occluded H_2BDC molecules) derived in two versions (with and without fluorine atoms linked to the framework, namely $Ga(OH)_{0.8}(F)_{0.2}(BDC)\cdot 0.74H_2BDC$ and $Ga(OH)(BDC)\cdot 0.74H_2BDC$, respectively) has been very recently reported by Jacobson and co-workers.[35] Single crystal X-ray analysis was performed on both compounds. Meanwhile, we conducted a similar study by highlighting an incommensurate structure which will be shown thereafter for the non-containing fluorine material.

Gallium(III) nitrate and terephthalic acid react in a HF mixture to yield a white crystalline solid IM-19 ps (ps: post-synthesis), $Ga(OH)(BDC)\cdot 0.75H_2BDC$.†[36] It is important to note that no fluorine was found by elemental analysis (detection threshold equal to 0.2 wt%) in contrast to Jacobson and co-workers report where the percentage of fluorine in their material is close to 1.2 wt%.[35] The substitution of occluded H_2BDC molecules by DMF molecules is achieved by a solvothermal treatment in DMF of IM-19 ps giving rise to IM-19 dmf, $Ga(OH)(BDC)\cdot 0.85DMF$.† The removal of DMF molecules is permitted by the heating of IM-19 dmf at 220 °C for 1 day under air. After cooling down to room temperature, atmospheric water molecules are trapped in the Ga(OH)(BDC) network leading to IM-19 h (h: hydrated), $Ga(OH)(BDC)\cdot H_2O$.†

Single crystal X-ray diffraction measurements were performed on IM-19 ps and IM-19 dmf. IM-19 ps is structurally related to MIL-53 as[30–32,35] (as: as-synthesized) and MIL-47[33] materials. However, as illustrated in Fig. 1(a) the (. *k l*)* layers of the parent material IM-19 ps exhibit additional Bragg peaks that cannot be simply indexed with the reciprocal vectors $\boldsymbol{a}^*$, $\boldsymbol{b}^*$, $\boldsymbol{c}^*$ associated with the usual lattice periodicity in orthorhombic symmetry ($a \sim 18$ Å, $b \sim 7$ Å, $c \sim 12$ Å) reported for MIL-53 and MIL-47 materials. Indeed, the diffraction pattern requires the introduction of a 4D superspace formalism,[37] where the main lattice reflections $h\boldsymbol{a}^* + k\boldsymbol{b}^* + l\boldsymbol{c}^* + 0\boldsymbol{q}$ are indexed on the basis of the orthorhombic unit-cell parameters (a = 17.4370(2) Å, b = 6.7475(4) Å, c = 12.1541(4) Å), and satellites $h\boldsymbol{a}^* + k\boldsymbol{b}^* + l\boldsymbol{c}^* + m\boldsymbol{q}$ are described using an incommensurate

[a] *Equipe Matériaux à Porosité Contrôlée (MPC), Institut de Science des Matériaux de Mulhouse (IS2M), LRC CNRS 7228, Université Haute Alsace, ENSCMu, 3 rue Alfred Werner, 68093, Mulhouse Cedex, France. E-mail: gerald.chaplais@uha.fr; Fax: +33 3 89 33 68 85; Tel: +33 3 89 33 68 87*
[b] *CEA, IRAMIS, Laboratoire Léon Brillouin, 91191 Gif sur Yvette, France. LLB, UMR 12 CEA-CNRS, 91191, Gif sur Yvette, France. E-mail: Florence.Porcher@cea.fr; Fax: +33 1 69 08 82 61; Tel: +33 1 69 08 49 54*
[c] *Cristallographie, Résonance Magnétique et Modélisations (CRM2), UMR 7036 CNRS-Université Henri Poincaré Nancy 1, Boulevard des Aiguillettes, BP 239, 54506, Vandoeuvre-lès-Nancy, France*
[d] *IFP-Lyon, BP 3, 69360, Solaize, France*

† Electronic supplementary information (ESI) available: Full synthesis details, TG curves and table summarizing crystallographic data for IM-19 phases and related materials. CCDC reference numbers 713193 and 713194. For ESI and crystallographic data in CIF or other electronic format see DOI: 10.1039/b822163d

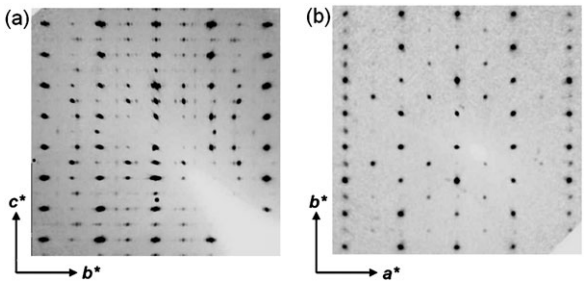

Fig. 1 Precession reconstruction of the (3 *k l*)* layer of IM-19 ps (a) and (*h k* 3)* layer of IM-19 dmf (b). For IM-19 dmf, the 4 *k* 3 Bragg spots that seem to violate the I-centering are explained by the twinning of the sample.

vector $\boldsymbol{q}$ = (0 0.104 0).[38] The strong modulation observed (satellites up to order m = 4 are visible) has to be related with the "composite" aspect of the structure where the Ga(OH)(BDC) framework is believed to interact strongly with the sub-lattice of the guest H_2BDC molecules.

Based on the mean structure, IM-19 ps (Ga(OH)(BDC)·0.75H_2BDC) consists of a three-dimensional framework which is formed of chains of gallium octahedra sharing OH vertices, running along the *b* axis and linked through the terephthalate moieties (Fig. 2(a)). Protonated terephthalic acid molecules fill the one-dimensional lozenge-shaped channels. The envelopes of H_2BDC molecules appear neatly on the difference Fourier maps reported in Fig. 3. A more precise description of the structure, including the guest terephthalic acid molecules using the superspace group formalism will be presented in a forthcoming paper.

For IM-19 dmf, in contrast to IM-19 ps, the precession image clearly shows no satellite reflections (Fig. 1(b)) and the hybrid can be described in the conventional 3D space. The substitution of the guest H_2BDC by DMF molecules comes along with a monoclinic distortion of the unit-cell with a = 6.7120(4) Å, b = 11.2486(11) Å, c = 17.9650(16) Å and β = 91.975(7)° inducing a twinning of the crystal (Fig. 2(b)). The symmetry changes from *Pnma* (mean structure approximation) for IM-19 ps to *I*2/*a* (conventional space group: *C*2/*c*) for IM-19 dmf. Within this approximation for IM-19 ps, the structure can be solved by direct methods[39] after merging of the main and satellite reflections, and its framework refined[40] down to R = 0.098, wR = 0.210 (main reflections only).

A X-ray thermodiffraction study carried out in air on IM-19 dmf as starting material from 25 to 350 °C, and depicted in

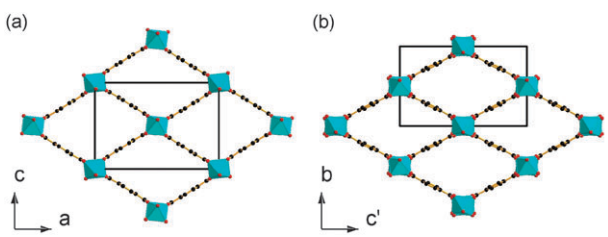

Fig. 2 Representations of the lozenge-shaped frameworks of IM-19 ps (a) and IM-19 dmf ((b): view along *a* axis, $c' = c\sin\beta$) (Ga: turquoise, O: red, C: black).

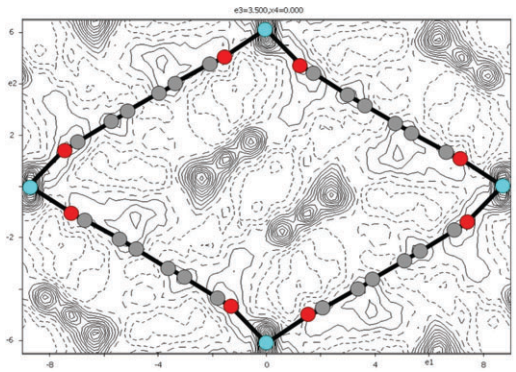

Fig. 3 Difference Fourier map in Ga(OH)(BDC)·0.75H_2BDC, IM-19 ps (mean structure described in *Pnma*, framework only), showing the envelopes of H_2BDC guest molecules (Ga: turquoise, O: red, C: grey). The electron density is projected in the (*a*, *c*) plane (contours 0.02 e Å^{-3}).

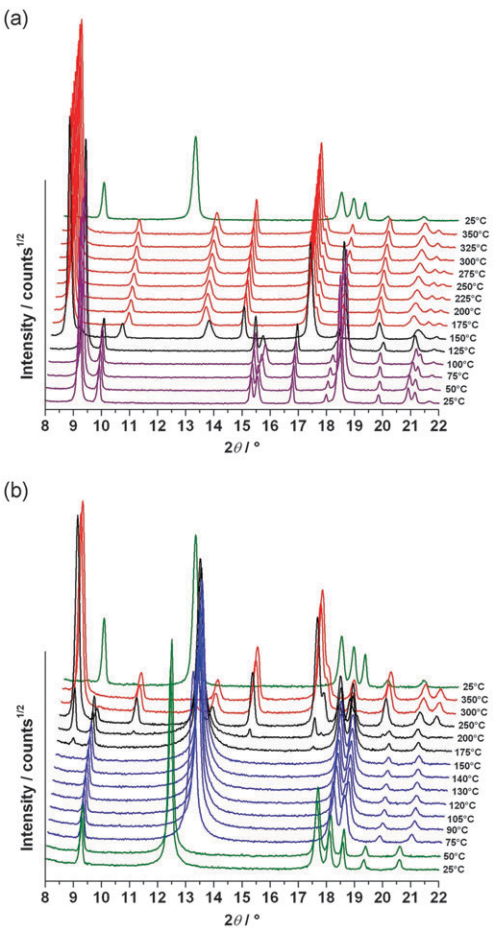

Fig. 4 X-Ray thermodiffraction patterns in air (25 to 350 °C) of IM-19 dmf (a) and IM-19 h (b) as starting materials (IM-19 dmf: purple, IM-19 p2: red, IM-19 h: green, IM-19 p1: blue, mixtures of phases: black).

Fig. 4(a), has highlighted the formation of a guest-free phase denoted IM-19 p2, Ga(OH)(BDC), at high temperatures (175 to 350 °C). The latter crystallizes at 350 °C in the following orthorhombic system: a = 16.7338(31) Å,

b = 13.2824(26) Å, c = 6.7413(9) Å, $M(20)$ = 35.3. After cooling down to room temperature (T = 25 °C) and rehydration in air, Ga(OH)(BDC)·H_2O (IM-19 h), is obtained and crystallizes in the monoclinic symmetry: a = 19.1866(26) Å, b = 7.6278(13) Å, c = 6.6688(7) Å, β = 95.858(10)°, Figure of Merit $M(20)$ = 34.6.

A similar experiment was realized with IM-19 h as starting material (Fig. 4(b)). The removal of water molecules leads to the formation of another guest-free phase, Ga(OH)(BDC), called IM-19 p1, with the following monoclinic unit-cell parameters at 140 °C: a = 19.3021(33) Å, b = 7.1577(15) Å, c = 6.7156(16) Å, β = 95.133(18)°, $M(20)$ = 23.9. Moreover, during the dehydration at higher temperatures (T > 250 °C), the framework expansion and the transformation into IM-19 p2 take place, making IM-19 p1 a metastable phase. Consequently, IM-19 p1 and IM-19 p2 can be considered as temperature-dependent polymorphs. After cooling down to room temperature and rehydration in air, IM-19 h is obtained, demonstrating that the dehydration–rehydration process is reversible.

In order to compare the expansion/shrinkage of the framework due to the inclusion/removal of guest molecules, the lozenge structural representation (Fig. 5) and calculation method, described by Férey and co-workers,[41] were adopted. The edge of lozenge represents the distance between two inorganic chains through the terephthalate ligands. The angle α value is determined from the unit-cell parameters by taking into account the crystallographic system and corresponds to the arctangent value of the d/D ratio. It symbolizes the framework deformation upon insertion/removal of guest molecules. Crystallographic data of the five IM-19 phases and those of other M(OH)(BDC) type materials (where M = Al, Cr, Fe, V, In) are summarized and classified by occluded molecules in the ESI.†

When H_2BDC, DMF or H_2O molecules fill the 1D channels, the framework of IM-19 hybrids undergoes some deformations comparable to those observed for other frameworks of M(OH)(BDC) materials. For loaded IM-19 frameworks, the highest expansion is observed when H_2BDC molecules are occluded (α = 34.9°) whereas the highest shrinkage occurs when H_2O molecules are occluded (α = 21.8°).† For IM-19 dmf, the α value is equal to 32.1°.† On the other hand, the main difference between the framework of IM-19 and that of other M(OH)(BDC) type materials appears for the guest-free phases. Indeed, IM-19 p1 which adopts a more shrunken structure than IM-19 h (α = 20.4°),

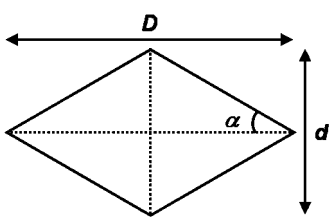

Fig. 5 Representation of 1D lozenge-shaped channel for the IM-19 hybrids and the related M(OH)(BDC) materials where M = Al, Cr, Fe, V.

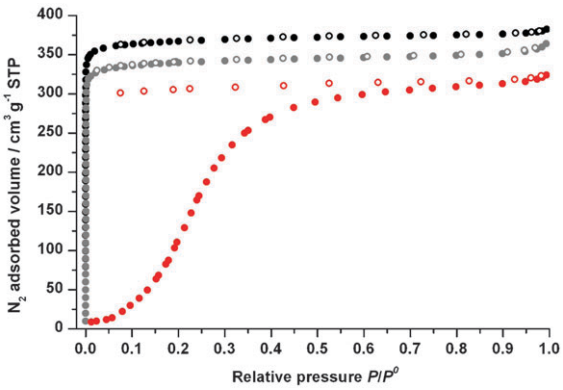

Fig. 6 Nitrogen sorption isotherms performed at 77 K of the dehydrated samples of MIL-53(Al), MIL-53(Cr) and IM-19 (black: MIL-53(Al), grey: MIL-53(Cr), red: IM-19, closed circles: adsorption, open circles: desorption).

has to be related to the closed form of MIL-53(Fe) (MIL-53(Fe) ht, ht: high temperature) and IM-19 p2, where α = 38.4°, exhibits an open structure similar to those encountered in MIL-53(Al) ht, MIL-53(Cr) ht and MIL-47.†

The textural features of the Ga(OH)(BDC) framework were also evaluated by nitrogen sorption measurements at 77 K and compared to the MIL-53(Al) and MIL-53(Cr) analogues, namely MIL-53(Al) ht and MIL-53(Cr) ht, respectively. Each dehydrated material was activated after outgassing at 200 °C for 12 hours under vacuum of the corresponding hydrated compound (IM-19 h as well as MIL-53(Al) and MIL-53(Cr) prepared according to the literature[30,31]). In contrast to the MIL-53 materials, an unusual isotherm is obtained for IM-19, especially for the adsorption branch as shown in Fig. 6. The non-profile I adsorption isotherm characterized by a very low nitrogen up-take at low relative pressures (P/P^0 < 0.07) can be explained by the predominance of the dehydrated and closed-shaped Ga(OH)(BDC) phase IM-19 p1. At higher relative pressures (0.07 < P/P^0 < 0.55), the framework opens progressively to tend finally to a porous polymorph. The gate-opening and the gate-closing pressures as defined by Kitagawa *et al.*[42] appear to be close to P/P^0 = 0.07 and P/P^0 = 0.55, respectively. Moreover, it is worth noting that the desorption branch is characterized by a plateau and shows no meaningful decrease of adsorbed nitrogen (classical type I desorption profile). The micropore volumes of 0.57 and 0.52 $cm^3\ g^{-1}$ determined for the MIL-53(Al) ht and MIL-53(Cr) ht samples, respectively, are in good agreement with previous reported values.[10] The corresponding BET surface areas reach 1517 and 1401 $m^2\ g^{-1}$.‡ For IM-19, the micropore volume is equal to 0.47 $cm^3\ g^{-1}$.‡ When the micropore volumes of these materials are based on the weight of M(OH)(BDC) unit, they become 117.8, 122.2 and 118.6 cm^3 per M(OH)(BDC) unit for MIL-53(Al) ht, MIL-53(Cr) ht and the guest-free and porous form of IM-19, respectively. These values reflect some close nitrogen sorption capacities (per M(OH)(BDC) unit) and therefore some high similarities for the pore topologies in the three analyzed materials. In addition, it has to be reminded that the expansion of the frameworks determined from crystallographic data for MIL-53(Al) ht, MIL-53(Cr) lt and IM-19 p2 are very close.†

Consequently, the guest-free and porous form of IM-19 evident by nitrogen sorption measurements can be assigned to IM-19 p2.

In conclusion, five gallium-containing MOFs (IM-19 hybrids) based on the lozenge-shaped Ga(OH)(BDC) framework have been described. For three of them, IM-19 ps, IM-19 dmf and IM-19 h (where ps, dmf and h refer to H_2BDC, DMF and H_2O occluded molecules, respectively), the framework undergoes an expansion/shrinkage phenomenon according to the nature of the guest molecules. For the first time, an incommensurate structure has been evident (IM-19 ps) for M(OH)(BDC) type materials (where M = Ga, Al, Cr, Fe, V, In) and is probably induced by a sub-lattice of ordered guest molecules.

The two other hybrids, IM-19 p1 and IM-19 p2, are guest-free polymorphs but show some significant differences. The former possesses a closed form whereas the latter is porous. In term of flexibility, IM-19 is believed to be an intermediate framework between the high breathing MIL-53(Al) and MIL-53(Cr) materials, on the one hand, and MIL-53(Fe), on the other hand. The remarkable flexibility upon the inclusion of guest molecules and the presence of hydroxyl groups makes the dynamic porous framework IM-19 a potential candidate for separation and catalytic applications.

References

‡ Single crystal X-ray diffraction measurements were performed at room temperature using graphite-monochromated Mo Kα radiation on an Oxford Diffraction Xcalibur diffractometer equipped with a bidimensional CCD detector. Diffraction data for IM-19 ps and IM-19 dmf were collected with a large redundancy (12.7 and 9.5, respectively, up to $\sin\theta/\lambda$ = 0.73 Å and 1.15 Å) in order to test the symmetry. CRYSALIS software[43] was used to analyze the diffraction frames (indexation, integration and reconstruction of precession images of the reciprocal space).

Crystal data for IM-19 ps, $0.5[Ga(OH)(O_2CC_6H_4CO_2)]\cdot 0.375HO_2CC_6H_4CO_2H$, M = 187.7 g mol^{-1}, orthorhombic system, space group *Pnma* (no. 62), a = 17.4370(2) Å, b = 6.7475(4) Å, c = 12.1541(4) Å, V = 1430.0(1) Å^3, Z = 8, D_c = 1.744 g cm^{-3}, T = 293 K, $F(000)$ = 754.0, 84 993 reflections measured, 9127 unique (R_{int} = 0.1162) from which 3875 with $I > 3\sigma(I)$ were used in all calculations. The final w$R(F^2)$ = 0.2113 (CCDC 713194). Crystal data for IM-19 dmf, $0.5[Ga(OH)(O_2CC_6H_4CO_2)]\cdot 0.425(CH_3)_2NCOH$, M = 156.5 g mol^{-1}, monoclinic system, space group $I2/a$ (conventional space group: $C2/c$, no. 15), a = 6.7120(4) Å, b = 11.249(1) Å, c = 17.965(2) Å, β = 91.975(7)°, V = 1355.6(2) Å^3, Z = 8, D_c = 1.534 g cm^{-3}, T = 293 K, $F(000)$ = 608.2, 22 796 reflections measured, 1779 unique (R_{int} = 0.1021) from which 1288 with $I > 3\sigma(I)$ were used in all calculations. The final w$R(F^2)$ = 0.1297 (CCDC 713193). The X-ray thermodiffraction studies were carried out upon air on a Panalytical X'Pert Pro apparatus equipped with a HTK 1200 high temperature oven chamber from Anton Paar. The nitrogen sorption measurements were performed on a Micromeritics ASAP 2420 apparatus. For MIL-53 samples, the micropore volumes were determined by the Dubinin–Radushkevich method. The BET surface areas were calculated according to the criteria given in the literature[44,45] in the $0.0002 < P/P^0 < 0.0200$ and $0.0006 < P/P^0 < 0.0200$ ranges for MIL-53(Al) ht and MIL-53(Cr) ht, respectively. For IM-19, the micropore volume is obtained by a single point determination at $P/P^0 \sim 0.2$ (pore diameters less than 20 Å) from the desorption branch.

1 B. Panella, M. Hirscher, H. Putter and U. Muller, *Adv. Funct. Mater.*, 2006, **16**, 520.
2 A. G. Wong-Foy, A. J. Matzger and O. M. Yaghi, *J. Am. Chem. Soc.*, 2006, **128**, 3494.
3 J. L. C. Rowsell and O. M. Yaghi, *J. Am. Chem. Soc.*, 2006, **128**, 1304.
4 H. K. Chae, D. Y. Siberio-Perez, J. Kim, Y. Go, M. Eddaoudi, A. J. Matzger, M. O'Keeffe and O. M. Yaghi, *Nature*, 2004, **427**, 523.
5 J. L. C. Rowsell, A. R. Millward, K. S. Park and O. M. Yaghi, *J. Am. Chem. Soc.*, 2004, **126**, 5666.
6 H. Furukawa, M. A. Miller and O. M. Yaghi, *J. Mater. Chem.*, 2007, **17**, 3197.
7 G. Férey, C. Mellot-Draznieks, C. Serre and F. Millange, *Acc. Chem. Res.*, 2005, **38**, 217.
8 G. Férey, C. Mellot-Draznieks, C. Serre, F. Millange, J. Dutour, S. Surblé and I. Margiolaki, *Science*, 2005, **309**, 2040.
9 P. Horcajada, C. Serre, M. Vallet-Regi, M. Sebban, F. Taulelle and G. Férey, *Angew. Chem., Int. Ed.*, 2006, **45**, 5974.
10 M. Latroche, S. Surblé, C. Serre, C. Mellot-Draznieks, P. L. Llewellyn, J. H. Lee, J. S. Chang, S. H. Jhung and G. Férey, *Angew. Chem., Int. Ed.*, 2006, **45**, 8227.
11 O. I. Lebedev, F. Millange, C. Serre, G. Van Tendeloo and G. Férey, *Chem. Mater.*, 2005, **17**, 6525.
12 D. F. Sun, S. Q. Ma, Y. X. Ke, D. J. Collins and H. C. Zhou, *J. Am. Chem. Soc.*, 2006, **128**, 3896.
13 G. Férey, *Chem. Soc. Rev.*, 2008, **37**, 191.
14 C. Paulet, C. Serre, T. Loiseau, D. Riou and G. Férey, *C. R. Acad. Sci., Ser. IIc: Chim.*, 1999, **2**, 631.
15 M. Bujoli-Doeuff, M. Evain, F. Fayon, B. Alonso, D. Massiot and B. Bujoli, *Eur. J. Inorg. Chem.*, 2000, 2497.
16 J. Morizzi, M. Hobday and C. Rix, *J. Mater. Chem.*, 2000, **10**, 1693.
17 M. Bujoli-Doeuff, M. Evain, P. Janvier, D. Massiot, A. Clearfield, Z. H. Gan and B. Bujoli, *Inorg. Chem.*, 2001, **40**, 6694.
18 T. Loiseau, S. Neeraj and A. K. Cheetham, *Acta Crystallogr., Sect. C*, 2002, **58**, m379.
19 H. G. Harvey, A. C. Herve, H. C. Hailes and M. P. Attfield, *Chem. Mater.*, 2004, **16**, 3756.
20 M. P. Attfield, H. G. Harvey and S. J. Teat, *J. Solid State Chem.*, 2004, **177**, 2951.
21 H. G. Harvey and M. P. Attfield, *Chem. Mater.*, 2004, **16**, 199.
22 C. H. Lin and K. H. Lii, *Inorg. Chem.*, 2004, **43**, 6403.
23 C. A. Merrill and A. K. Cheetham, *Inorg. Chem.*, 2005, **44**, 5273.
24 F. Fredoueil, D. Massiot, D. Poojary, M. Bujoli-Doeuff, A. Clearfield and B. Bujoli, *Chem. Commun.*, 1998, 175.
25 T. Loiseau, H. Muguerra, M. Haouas, F. Taulelle and G. Férey, *Solid State Sci.*, 2005, **7**, 603.
26 C. Volkringer, T. Loiseau, G. Férey, C. M. Morais, F. Taulelle, V. Montouillout and D. Massiot, *Microporous Mesoporous Mater.*, 2007, **105**, 111.
27 C. Volkringer, M. Meddouri, T. Loiseau, N. Guillou, J. Marrot, G. Férey, M. Haouas, F. Taulelle, N. Audebrand and M. Latroche, *Inorg. Chem.*, 2008, **47**, 11892.
28 P. Caullet, J.-L. Paillaud, A. Simon-Masseron, M. Soulard and J. Patarin, *C. R. Chim.*, 2005, **8**, 245.
29 J. Patarin, J.-L. Paillaud and H. Kessler, in *Handbook of Porous Solids*, ed. F. Schüth, K. S. W. Sing and J. Weitkamp, Wiley-VCH, Weinheim, Germany, 2001, vol. 2, p. 815.
30 T. Loiseau, C. Serre, C. Huguenard, G. Fink, F. Taulelle, M. Henry, T. Bataille and G. Férey, *Chem.–Eur. J.*, 2004, **10**, 1373.
31 C. Serre, F. Millange, C. Thouvenot, M. Nogues, G. Marsolier, D. Louer and G. Férey, *J. Am. Chem. Soc.*, 2002, **124**, 13519.
32 F. Millange, C. Serre and G. Férey, *Chem. Commun.*, 2002, 822.
33 K. Barthelet, J. Marrot, D. Riou and G. Férey, *Angew. Chem., Int. Ed.*, 2002, **41**, 281.
34 S. Kitagawa and K. Uemura, *Chem. Soc. Rev.*, 2005, **34**, 109.
35 M. Vougo-Zanda, J. Huang, E. Anokhina, X. Wang and A. J. Jacobson, *Inorg. Chem.*, 2008, **47**, 11535.
36 G. Chaplais, A. Simon-Masseron, J. Patarin, N. Bats and D. Bazer-Bachi, FR Pat., 08/01.089, 2008.
37 P. M. Dewolff, T. Janssen and A. Janner, *Acta Crystallogr., Sect. A*, 1981, **37**, 625.
38 A. Schonleber, M. Meyer and G. Chapuis, *J. Appl. Crystallogr.*, 2001, **34**, 777.
39 M. C. Burla, R. Caliandro, M. Camalli, B. Carrozzini, G. L. Cascarano, L. De Caro, C. Giacovazzo, G. Polidori and R. Spagna, *J. Appl. Crystallogr.*, 2005, **38**, 381.

40 *Jana2006*. *The crystallographic computing system*, Institute of Physics, Praha, Czech Republic, 2006.
41 F. Millange, C. Serre, N. Guillou, G. Férey and R. I. Walton, *Angew. Chem., Int. Ed.*, 2008, **47**, 4100.
42 S. Kitagawa, R. Kitaura and S. Noro, *Angew. Chem., Int. Ed.*, 2004, **43**, 2334.
43 *Oxford Diffraction*, Oxford Diffraction Ltd., Xcalibur CCD system, CrysAlisPro Software system, 2007.
44 K. S. Walton and R. Q. Snurr, *J. Am. Chem. Soc.*, 2007, **129**, 8552.
45 J. Rouquerol, P. Llewellyn and F. Rouquerol, *Stud. Surf. Sci. Catal.*, 2007, **160**, 49.